Journal of Water Sciences Research
ISSN: 2251-7405 eISSN: 2251-7413
Vol.4, No.1, Fall 2012, 19-29, JWSR

JWSR

Sensitivity Analysis of Mike21-BW Diffraction Model by using Breakwater Reflection Coefficient

H.Rabiefar[1*],A. Akbarpour[2], M. Pourlak[3]

1,2. Assistant Professor, Department of Civil Engineering, Islamic Azad University-South Tehran Branch, Tehran, Iran
3.M.Sc. in Civil Engineering, Hydraulic Structures, Member of Young Researchers Club - Islamic Azad University South Tehran Branch, Tehran, Iran

Received: 8 Fav. 2012 Accepted: 30 Jun 2012

ABSTRACT

DHI-Mike Software is one of best softwares describing water wave diffraction in onshore/offshore concepts. Diffraction happens due to obstacles along wave direction and has an important role in designing structures. The scope of this study is to show the relation between Porosity Coefficient and its effects on Diffraction Coefficient (C_d) by means of a suitable and verified numerical model. Porosity Coefficient is one of the breakwaters' characteristics that describe the reflection quantity of the wave that influences on Diffraction Coefficient. This parameter determines the quantity of obstacles porosity and helps in implementing the sensitivity analysis. A calibrated Model helps as a suitable background to examine different Porosity Coefficients. Reputed "Wave Diffraction Diagrams" has been used for model calibration and will be discussed in detail in an appropriate section. It has been concluded that by increasing the Porosity Coefficient, wave height and Diffraction Coefficient increase.

Keywords

Diffraction; Sensitivity Analysis; Porosity Coefficient; Reflection Coefficient; DHI-MIKE 21; Boussinesq Wave Equations

1.Introduction

Diffraction refers to various phenomena which occur when a wave encounters an obstacle. It is described as the apparent bending of waves around small obstacles and the spreading out of waves past small openings (Boussinesq 1872) .

While diffraction occurs propagating waves encounter obstacle, its effects are generally seen like changes on wavelength, wave height and wave propagating direction. Based on obstructing object size, type, porosity and other characteristics, provides multiple variety of diffraction intensity (Sorenson 2006).

Parameters that may influence the diffraction phenomenon vary. Reflection Coefficient (R_f) describes the amount of wave height that a substance reflects. Meanwhile, Porosity Coefficient (P_c) has same meaning in reverse order. Porosity Coefficient is the substance characteristics which describes its porous mood. Usually, by increasing the reflection ability of a substance its Porosity Coefficient will decreases and vice versa.

Diffraction occurs because of the way in which waves propagate; this is described by the Huygens–Fresnel lemma. The propagation of a wave can become tangible by

* Corresponding Author Email: (Rabiefar@yahoo.com)

considering every point on a wave front as a node in computer modeling (Kim and lee 2009). The subsequent propagation and addition of all these waves form the new wave. When waves added together, the result is determined by the relative phases as well as the amplitudes of the individual waves. The summed amplitude of the waves can have any value between zero and the sum of the individual waves. Thus, diffraction patterns usually have a series of maxima and minima.

The form of a diffraction pattern can be resulted from the summation of the phases and amplitudes of the Huygens wavelets at each point in space. There are various analytical models which have the ability of doing this, including the Fraunhofer Diff-raction Equation for the far zone and the Fresnel Diffraction Equation for the near shore. Most formations including what mentioned in this paper could not be solved analytically easily, but can yield numerical solutions through FEM (Finite Element) and Boundary Elements Methods.

Boussinesq approximation for water waves is a valid one for nonlinear and long waves. The approximation name "Boussinesq", who first derived this (1872) in response to the observation by John Scott Russell, and named it as the Boussinesq equations (Boussinesq 1872; Sorenson et al. 2004; Sorenson et al. 1998; Madsen et al. 1997a). Subsequently, in 1872, Boussinesq derived the equations known nowadays as the Boussinesq equations (Madsen et al. 1991).

The Boussinesq approximation for water waves consider as the vertical structure of the horizontal and vertical flow velocity. This results in nonlinear partial differential equations which incorporate frequency. In coastal engineering, Boussinesq type equations are frequently used in computer models for the simulation of water waves in shallow waters: (Abbott et al. 1984; Gierlevsen et al. 2003).

The most important idea in Boussinesq approximation is the elimination of the vertical coordinate term from the flow equations, while hold some of the influences under water flow at vertical situation. As the waves propagate in the horizontal plane, this is useful and have a different -not usual- behavior in the vertical direction. Often the interest is primarily in the wave propagation: (Madsen et al. 1997b; Madsen et al. 1992).

2. Boussinesq Equations

Boussinesq approximation has different default assumptions that can be explained as:

A Taylor expansion in this appro-ximation is made of vertical and horizontal flow velocity in certain elevation. For approxi-mation, the mentioned Taylor expansion truncated to have a finite number of terms.

To replace vertical partial derivatives of quantities in the Taylor expansion with horizontal partial derivatives, Continuity Equation for incompressible flow and the zero curl condition for an irrotational flow are assumed (Boussinesq 1872; Madsen et al. 1992).

Thus, the Boussinesq approximation is applied to the remaining equations to eliminate the dependence on the vertical coordinate.

Therefore, the resulting Partial Differential Equations (PDE) are in terms of some functions that consist of the horizontal coor-dinates and also time (Sorenson et al. 2004; Madsen and Sorensen 1992).

As an example, consider potential flow over a horizontal datum in the (x,z) plane. Consider x (the horizontal) and z (the vertical coordinate). Consider z = -h the

bed, that h is the "Mean Water Depth".

In the Taylor expansion velocity potential φ(x,z,t) assumed at the bed level (z = -h), Eq. (1) (Boussinesq 1872).

$$\varphi = \varphi_b + z\left[\frac{\partial\varphi}{\partial z}\right]_{z=-h} + \frac{1}{2}z^2\left[\frac{\partial^2\varphi}{\partial x^2}\right]_{z=-h} + \frac{1}{6}z^3\left[\frac{\partial^3\varphi}{\partial x^3}\right]_{z=-h} + \frac{1}{24}z^4\left[\frac{\partial^4\varphi}{\partial x^4}\right]_{z=-h} + \ldots \quad (1)$$

Where $\varphi_b(x,t)$ is the velocity potential at z = -h. Using Laplace equation for φ, with the primary condition of validation for income-pressible flows, results in Eq. (2) (Boussinesq 1872).

$$\varphi = \left\{\varphi_b - \frac{1}{2}z^2\frac{\partial^2\varphi_b}{\partial x^2} + \frac{1}{24}z^4\frac{\partial^4\varphi_b}{\partial x^4} + \ldots\right\} + \left\{z\left[\frac{\partial\varphi}{\partial z}\right]_{z=-h} - \frac{1}{6}z^3\frac{\partial^2\varphi}{\partial x^2}\left[\frac{\partial\varphi}{\partial z}\right]_{z=-h} + \ldots\right\}$$
$$= \left\{\varphi_b - \frac{1}{2}z^2\frac{\partial^2\varphi_b}{\partial x^2} + \frac{1}{24}z^4\frac{\partial^4\varphi_b}{\partial x^4} + \ldots\right\} \quad (2)$$

The vertical velocity ∂φ/∂z at the imper-meable horizontal datum (z = -h) is zero. This series can be truncated to a finite number of terms as it has been mentioned in default assumptions.

Eqs. (3 and 4) are the boundary conditions at the free surface elevation z = η (x,t) for water waves on an incompressible fluid and irrotational flow in the (x,z) plane (Boussinesq 1872; Boussinesq 1872).

$$\frac{\partial\eta}{\partial t} + u\frac{\partial\eta}{\partial x} - w = 0 \quad (3)$$

$$\frac{\partial\varphi}{\partial t} + \frac{1}{2}(u^2 + w^2) + g\eta = 0 \quad (4)$$

Where g is the acceleration caused by gravity, u is the horizontal flow velocity component (u = ∂φ/∂x) and w is the vertical flow velocity component (w = ∂φ/∂z).

Now the Boussinesq approximation for the velocity potential (φ) is applied with assumption of these boundary conditions.

3. Numerical Model

3.1. Numerical Model Characteristics

The Model Contains 100×100meshes with a 5×5 grids and a horizontal opening in the middle of the model as shown in the fig. 1. Detailed model characteristics are described in table 1.

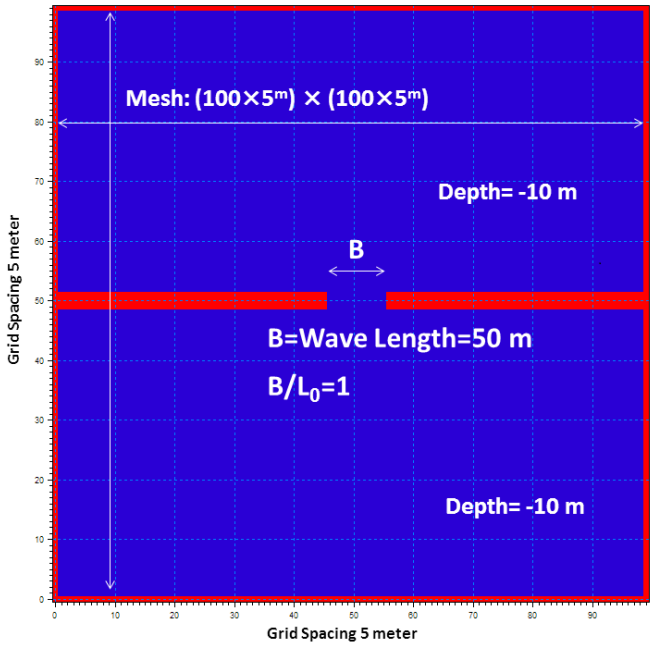

Fig. 1. Gridlines and Model Interface

As seen in fig. 2, the L_0 and B determined to get a verified model just like ''Diffraction Diagram'' mentioned in (USACE-CERC 1984) and (USACE-CEM 1998), with minimal inconstancy. Verification of the model for Running period tested for 15, 20, 25, 30, 35 and 40 minutes runs, and results are shown in fig. 3.

3.2. Running Verified Models

The models contain similar situations except the Porosity Coefficient to shows sensitivity to this parameter:

- Diffraction Coefficient calculation will be done by measuring specific nodes as shown in fig. 4.
- Results related to the Porosity of 0.85 are shown in fig. 5, as an example.

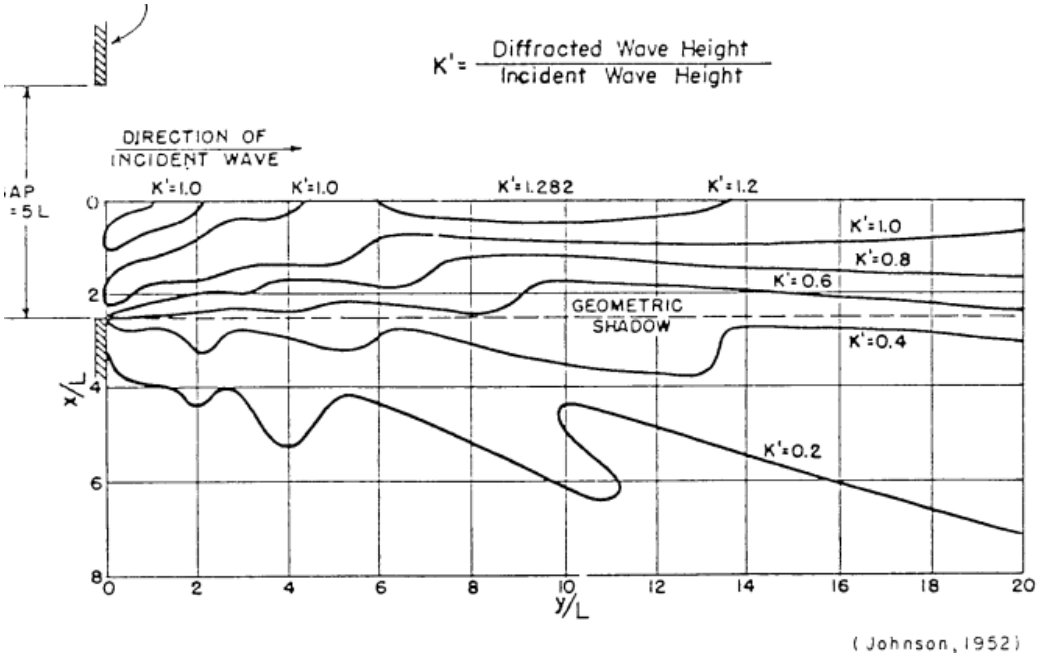

Fig. 2. Contours of equal Diffraction Coefficient gap width = 1 wavelength (B/L = 1), (SPM, 1984) and (CEM, 1998).

Table 1. Model Characteristics

	Details
Internal Wave Generation	JOHNSWAP Spectrum
T_p (Rayleighdistribution)	5.9581 Sec.
Run Period	15 min
Intervals	0.2 Sec.
Max Courant No.	0.396384
No. of Sponge Layers	10
Base Value	7
Power Value	0.7
Number of Porosity Layers	3
Value of Porosity	Varies (0.5~1.0)
Warm-up Period	283 Steps
L_0	50 m
T_s	5.66 Sec.
B (Breakwater opening width)	50 m
d (Depth)	-10 m

These nodes have "L_0 related" dimension in horizontal and vertical coordinates. "A" series determine zero distance from middle of the breakwater opening. "B" Series determine L_0 distance from the middle, "C" Series determine $2\times L_0$, and finally "D" Series represent $3\times L_0$.

In the same way, there are five horizontal series show $0\times L_0$, $1\times L_0$, $2\times L_0$, $3\times L_0$, $4\times L_0$ distance from the breakwater arm.The model will be run with specific characteristics shown in tables 1 and 2, and gives us raw data of each model. By obtaining Diffraction Coefficients from the result files, the phenomenon becomes more tangible (table 3).

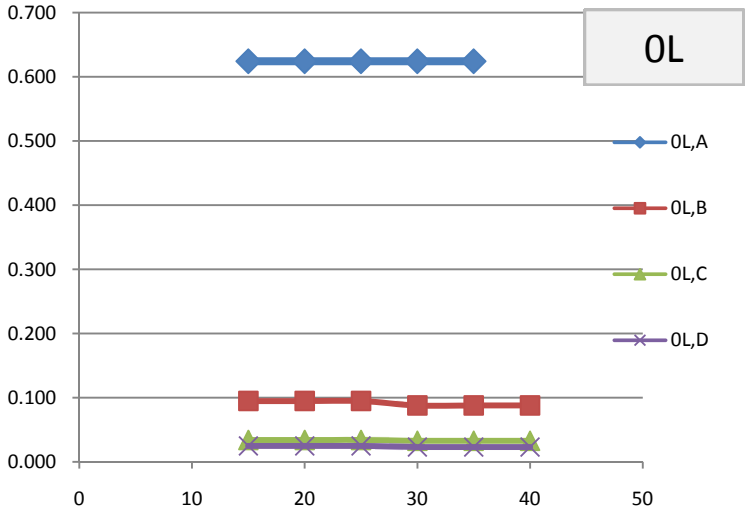

Fig. 3. Model Verification for Run Period

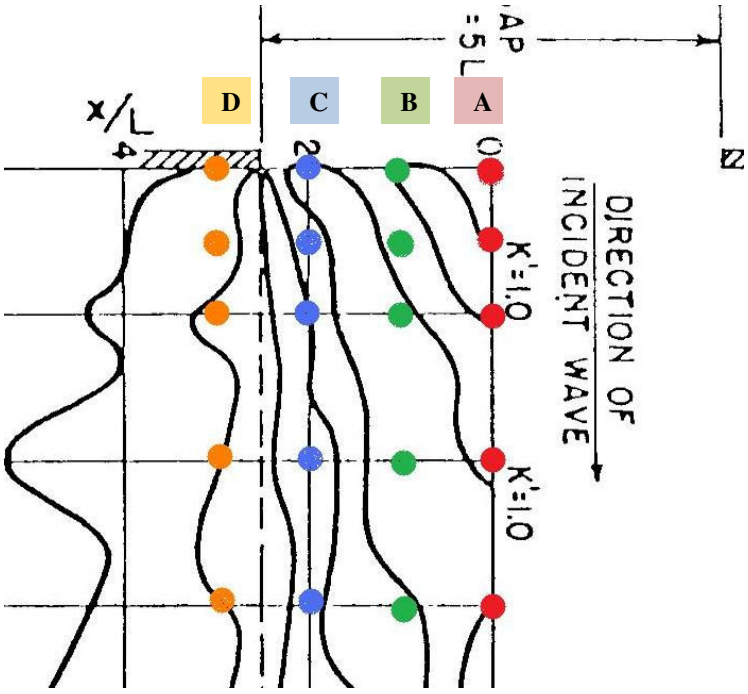

Fig. 4. Specific Measuring Nodes

Table 2.Values of Porosity

Model	Values of Porosity (0.5~1.0)
1	0.5
2	0.55
3	0.6
4	0.65
5	0.7
6	0.75
7	0.8
8	0.85
9	0.9
10	0.95
11	1.0

Table 3.Models Raw Data

Porosity Coeff.	Distance from the Opening	A Series	B Series	C Series	D Series
	0 L	0.7034	0.6034	0.3686	0.2416
	1 L	0.5424	0.4835	0.3822	0.2816
1.0	2 L	0.4179	0.4012	0.3662	0.3223
	3 L	0.3483	0.3407	0.3246	0.3025
	4 L	0.0140	0.0138	0.0134	0.0127
	0 L	0.9279	0.8628	0.5758	0.3761
	1 L	0.7316	0.6422	0.4950	0.3591
0.95	2 L	0.5805	0.5530	0.4951	0.4254
	3 L	0.4885	0.4763	0.4489	0.4099
	4 L	0.0193	0.0190	0.0184	0.0174
	0 L	0.8028	0.7028	0.4467	0.2896
	1 L	0.6099	0.5414	0.4243	0.3103
0.90	2 L	0.4770	0.4566	0.4139	0.3609
	3 L	0.3992	0.3900	0.3701	0.3420
	4 L	0.0160	0.0157	0.0152	0.0145
	0 L	0.7034	0.6034	0.3686	0.2416
	1 L	0.5424	0.4835	0.3822	0.2816
0.85	2 L	0.4179	0.4012	0.3662	0.3223
	3 L	0.3483	0.3407	0.3246	0.3025
	4 L	0.0140	0.0138	0.0134	0.0127
	0 L	0.6341	0.5341	0.3154	0.2102
	1 L	0.5012	0.4470	0.3547	0.2634
0.80	2 L	0.3802	0.3657	0.3353	0.2970
	3 L	0.3158	0.3091	0.2955	0.2769
	4 L	0.0126	0.0125	0.0121	0.0116
	0 L	0.5829	0.4829	0.2764	0.1874
	1 L	0.4754	0.4232	0.3364	0.2519
0.75	2 L	0.3550	0.3419	0.3144	0.2798
	3 L	0.2940	0.2879	0.2758	0.2597
	4 L	0.0117	0.0116	0.0112	0.0107
	0 L	0.5434	0.4434	0.2465	0.1697
	1 L	0.4599	0.4080	0.3248	0.2453
0.70	2 L	0.3381	0.3259	0.3004	0.2684
	3 L	0.2792	0.2735	0.2624	0.2482
	4 L	0.0110	0.0109	0.0106	0.0102
	0 L	0.5120	0.4120	0.2227	0.1550
	1 L	0.4522	0.3996	0.3183	0.2459
0.65	2 L	0.3273	0.3157	0.2914	0.2614
	3 L	0.2694	0.2641	0.2536	0.2409
	4 L	0.0106	0.0105	0.0102	0.0098
	0 L	0.4865	0.3865	0.2031	0.1422
	1 L	0.4569	0.3995	0.3165	0.2441
0.60	2 L	0.3212	0.3102	0.2866	0.2581
	3 L	0.2636	0.2587	0.2486	0.2370
	4 L	0.0103	0.0102	0.0099	0.0095
	0 L	0.4650	0.3650	0.1864	0.1304
	1 L	0.4450	0.3982	0.3151	0.2337
0.55	2 L	0.3191	0.3085	0.2854	0.2580
	3 L	0.2610	0.2564	0.2466	0.2360
	4 L	0.0101	0.0100	0.0097	0.0093
	0 L	0.4464	0.3464	0.1716	0.1190
	1 L	0.4355	0.3802	0.3054	0.2267
0.50	2 L	0.3204	0.3101	0.2874	0.2607
	3 L	0.2611	0.2570	0.2472	0.2376
	4 L	0.0100	0.0099	0.0096	0.0092

4. Data Analysis

Data analysis on table 3 is in two chart series. In both series there is the Diffraction Coefficient in vertical coordinate, and in first series horizontal coordinate represents vertical distance from breakwater in number of L_0 for every "A", "B", "C" and "D" series (fig. 6). In Second chart, horizontal coordinate reveals the Porosity Coefficient (fig. 7), (Madsen et al. 1983a and b; Ming et al. 1987)

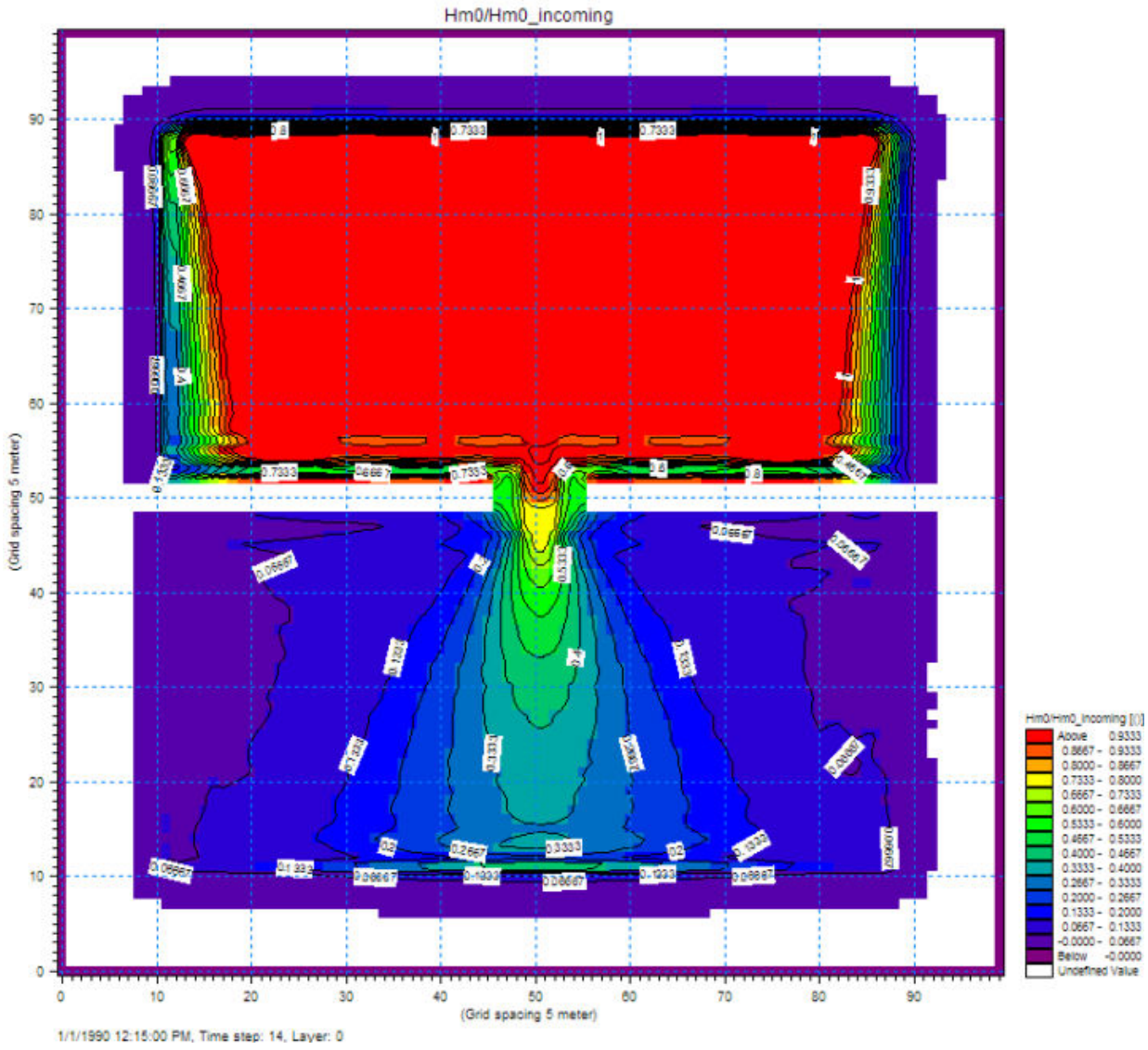

Fig. 5. Sample Run Result for Porosity Coefficient of 0.85

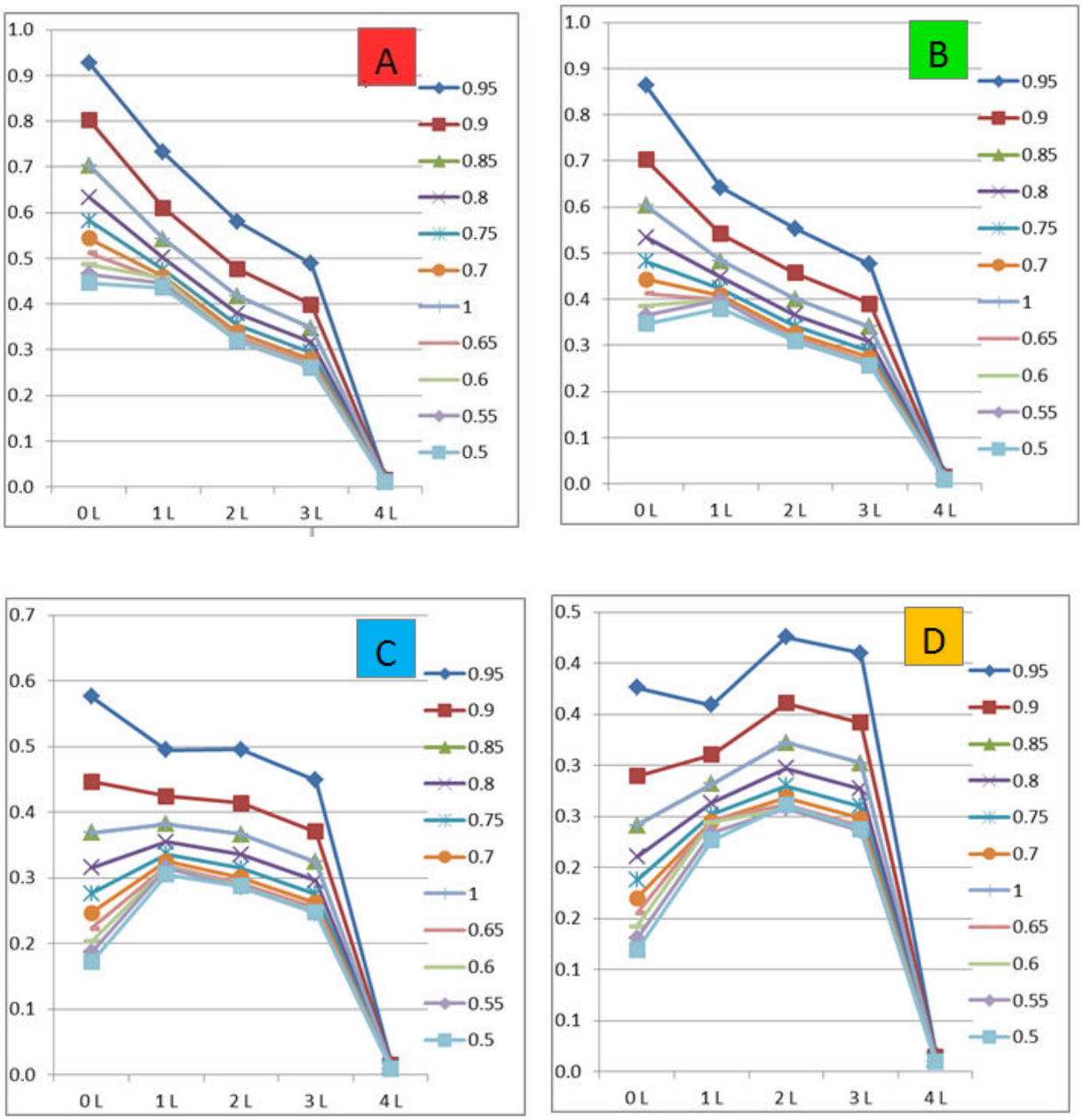

Fig. 6. A to D Data Analysis

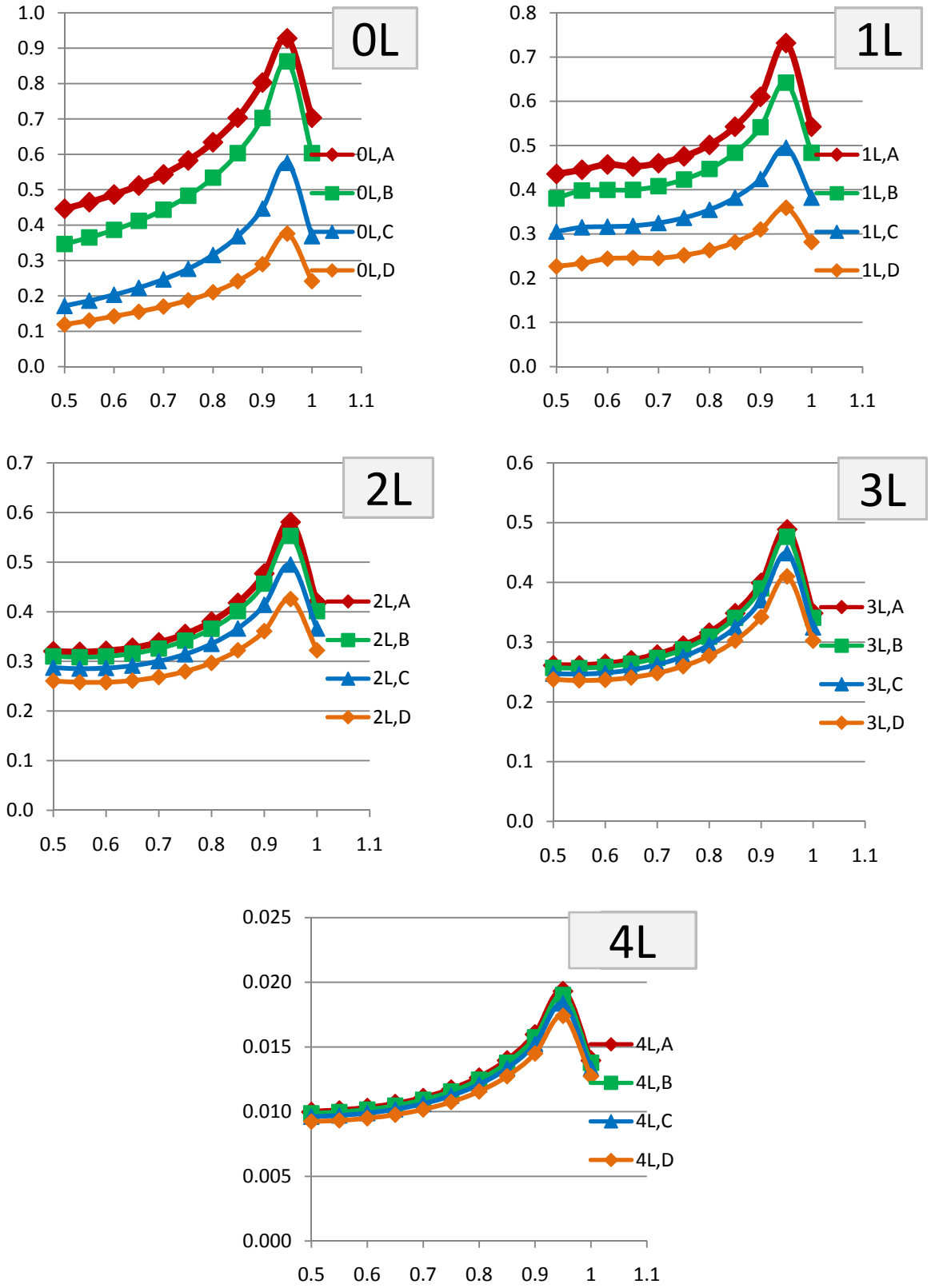

Fig. 7. Second Data Analysis

5. Conclusion

By means of suitable and verified numerical model the relation between Reflection Coefficient and the effects on Diffraction Coefficient has been revealed. Porosity Coefficient is what shows quantity of obstacles porosity which helps to determine this sensitive analysis and either is a one of breakwaters' characteristics than describes the reflection quantity of the wave that has influence on Diffraction Coefficient. Using these 11 models and analyzing their data a few conclusions can be made. By increasing of Reflection Coefficient (R_f) the Diffraction Coefficient (C_d) will reduce (for specific node). It means that by using materials which has more porous characteristics, Diffraction Coefficient will increases. This is a predictable result that shows this relation between these two integers.

Naturally for each series (A, B, C and D), C_d will reduce by increasing the distance from the middle of opening. Then by going forward from the opening to the shore, quantity of wave height and its index (C_d) will decrease.

For parameter less than 0.60 (for B Series), 0.85 (for C Series) and 0.90 (for D Series), there is different behavior of C_d. It means before these nodes there is usual mood for chart, but in the first node (0L, which is in the middle of the opening) it has ascending mood and in next node it becomes as usual.

In D series, the nodes set onto have ascending behavior instead of former descending estate. That shows because of more horizontal distance from the opening the effect of the parameter changes and instead of going toward less C_d it grows up.

It is easily deducted, by increasing the Porosity Coefficient (P_c) and decreasing Reflection Coeff. (R_f), the C_d, will increases in all horizontal profiles. That means that in the constant distance from the opening by increasing P_c, increasing of C_d has been observed.

The only different is in Porosity Coeff. =1 that cause the model quite a bit reduction in C_d in all Models. This reduction is because of natural effect of this quantity.

6. Acknowledgement

Special thanks to the DHI Company, who provide this research team with a research license of MIKE Software.

References

Abbott M.B., McCowan A.D., Warren I.R. (1984) Accuracy of Short-wave Numerical" Models. J. Hydr. Eng., 110: 173-197.

Boussinesq J. (1872) Théorie des ondes et des remous qui se propagent le long d'un canal rectangulaire horizontal, en communiquant au liquidecontenudansce canal des vitessessensiblementpareilles de la surface au fond. Journal de MathématiquesPures et Appliquées. DeuxièmeSérie, 17: 55–108.

Gierlevsen T., Vargas B.M., Pires V.P.L, Acetta D.J. (2003) Numerical and physical modeling of storm waves at Rio de Janeiro Yacht Club. In Proc. COPEDEC VI, Colombo, Sri Lanka, 17 pp.

Kim S.D. and Lee H.J. (2009) Diffraction Analysis by Gap Type Breakwater Using Polynomial Approximation for Fresnel Integral. European Journal of Scientific Research, 37(1): 85-93.

Ming K., AKej Y.M.R. (1987) Numerical modelling of harbour disturbance in comparison with physical modeling and field measurements. Proc. Second Int. Conf. on Coastal and Port Eng. in Developing Countries, Beijing, China.

Madsen, P A (1983a) Wave reflection from a vertical permeable wave absorber. Coastal

Eng., 7: 381-396.

Madsen P.A., Warren I.R. (1983b) Performance of a Short-wave Numerical Model. Coastal Engineering.

Madsen P.A., Sorensen O.R. (1992) A new form of the Boussinesq equations with improved linear dispersion characteristics. Part 2: A slowly-varying Bathymetry. Coastal Eng., 18: 183-204.

Madsen P.A., Murray R., Sorensen O.R. (1991) A new form of the Boussinesq equations with improved linear dispersion characteristics (Part 1). Coastal Eng., 15: 371-388.

Madsen P.A., Sorensen O.R., Schaffer H.A. (1997a) Surf zone dynamics simulated by a Boussinesq type model. Part I: Model description and cross-shore motion of regular waves. Coastal Eng., 32: 255-288.

Madsen P.A., Sorensen O.R., Schaffer H.A. (1997b) Surf zone dynamics simulated by a Boussinesq type model. Part II: Surf beat and swash zone oscillations for wave groups and irregular waves. Coastal Eng., 32: 289-320.

Sorensen R.M. (2006) Basic Coastal Engineering, Vol.1

Sorensen, O R, Schaffer, H A and Madsen P A (1998), Surf zone dynamics simulated by a Boussinesq type model. Part III: Wave-induced horizontal near shore circulations , Coastal Eng., 33, 155-176.

Sorensen, O R, Schaffer, H A and Sorensen.L S (2004). Boussinesq-type modeling using an unstructured finite element technique , Coastal Eng., 50, 181-198.

USACE-CEM (1998) Coastal Engineering Manual. Harbor hydrodynamics, II 7, 1998.

USACE-CERC (1984) Shore Protection Manual. Us Army Corps of Engineers, 1 & 2: 1984.